



Tomographic Imaging of Microelectronic Devices

John O'Sullivan, University College London, United Kingdom

September 4, 2019

Abstract

Avizo for FEI Systems is used to reconstruct in three-dimensions a microchip from a dataset of images produced using a FEI Focused Ion Beam (FIB)/Scanning Electron Microscope (SEM). Various filtering composites and image segmentation techniques are used to render the most precise reconstruction of the sample. The advantages and disadvantages of this method are discussed. Expansions on this technique, such as the integration of Energy-dispersive X-ray spectroscopy (EDX) are also explored.

Contents

1	Introduction	1
2	Materials and Methods	1
2.1	Image Processing	1
2.2	Image Alignment	1
2.3	Composite Image Filtering	2
2.4	Image Segmentation	3
3	Results & Analysis	5
3.1	Features of Interest	5
3.2	Volume Fraction V_f	6
3.3	Application to an Larger Sample	8
3.4	Limitations	8
4	Conclusions and Outlook	9

1 Introduction

Avizo for FEI Systems[1] is used to reconstruct in three-dimensions a microchip from a dataset of images produced using a FEI Focused Ion Beam (FIB)/Scanning Electron Microscope (SEM).

2 Materials and Methods

2.1 Image Processing

The images are obtained using the *Auto Slice & View 4* feature of the Focused Ion Beam FIB/SEM. The sample is milled at a depth of 20 nm per slice using a FIB. A image is taken of each of the 80 slices using the SEM, which are then saved as **TIFF** files (Figure 1). The slices are opened in *Avizo* and visualised using the **Ortho Slice** module, which

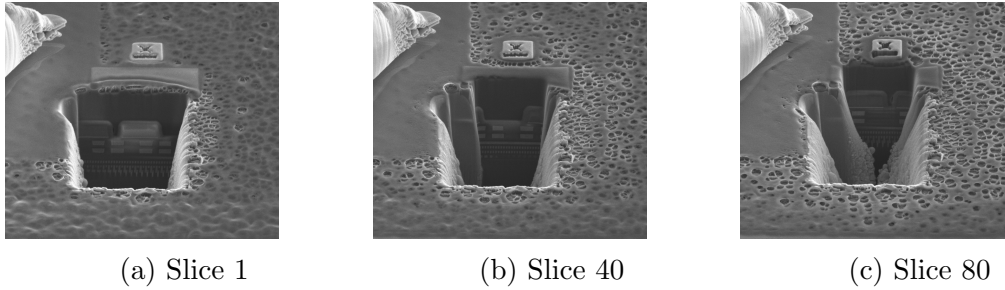


Figure 1: Slices of microchip sample milled using a FEI FIB

assigns each slice with integer values from 0 to 79 and displays them sequentially as an image stack in the *Project View*.

The **DualBeam 3D Wizard** module is used to process the images. This module compensates for the 52° stage tilt, align slices, reduce noise, reduce curtaining effect, correct intensity and crop the image to the desired area of interest.

However, with the samples, it was noted that this alignment technique was not sufficient to fully correct for the tilt. Initial reconstructions of the sample showed a tilt of exactly 52° , thus the next step was introduced to correct for this.

2.2 Image Alignment

The image stack is aligned using the **Align Slices** Module. This module allows the user to interactively align 2D slices of a 3D image stack. Alignment is performed in a separate graphics window that is activated by pressing the *Edit* button of the module's Action port.

The align window displays by default two consecutive slices using different draw styles that can be selected from the View menu. The two displayed slices can be chosen using the slice slider on the toolbar. Only one of these two slices is editable at a given time.

The slice that can be edited is selectable and it can be either the lower or the upper one. By dragging the editable slice using the left mouse button, the slice will be translated. The slice can be rotated around its centre by dragging it while keeping the middle mouse button pressed. At any time the numbers of the current slice pair as well as the quality of the current alignment is displayed in the status bar at the bottom of the align window. The quality value is based on the sum of squared gray-value difference (SSD) between the two slices being aligned. The SSD is computed for all pixels in the area in which the two slices overlap (the size of this area depends on the transformation of the slices). The SSD is then normed, so that it lies between 0 and 1. The quality in alignSlices is 1 minus this value, and therefore also lies between 0 and 1.

To close the slice aligner after alignment is complete, press the *Close* button of the module's *Action* port.

2.3 Composite Image Filtering

The image stack is then filter by a variety of different filters in a defined sequence, i.e. a “composite” of filters; including the **Sobel Filter**, the **Median Filter**, the **Bilateral Filter**, the **Arithmetic** module and the **Delineate** module. A sample The **Median Filter** Module is used to process the slices (Figure 2, Figure 3). This module uses lowpass filters to reduce the contrast and soften the edges of objects in the slices. The value of 3 is specified in the *Iterations* port, and *Interpretation* set to 3D.

The other filters work in a similar, manner, and the order of operations is shown in Figure 4.

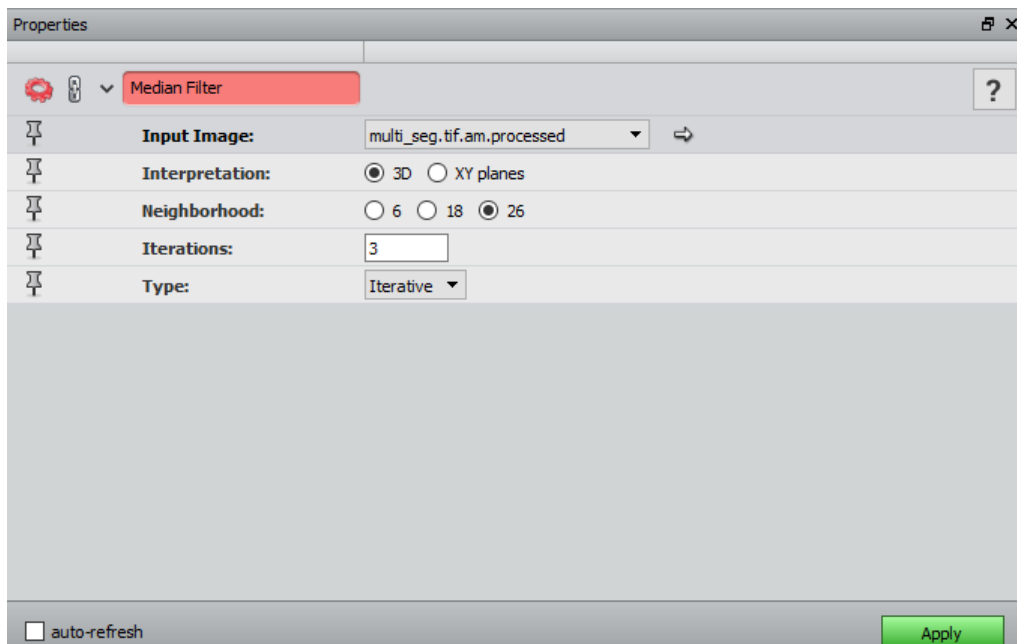


Figure 2: The Properties Area of the **Median Filter** module.

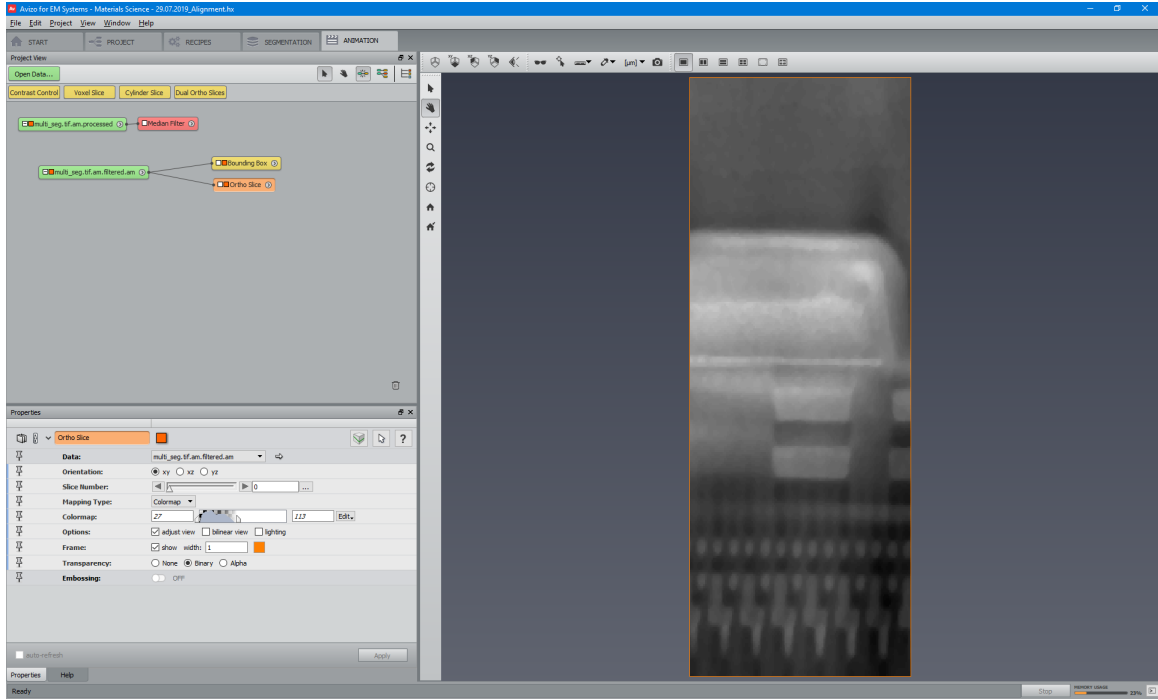


Figure 3: Result of the Median Filter module

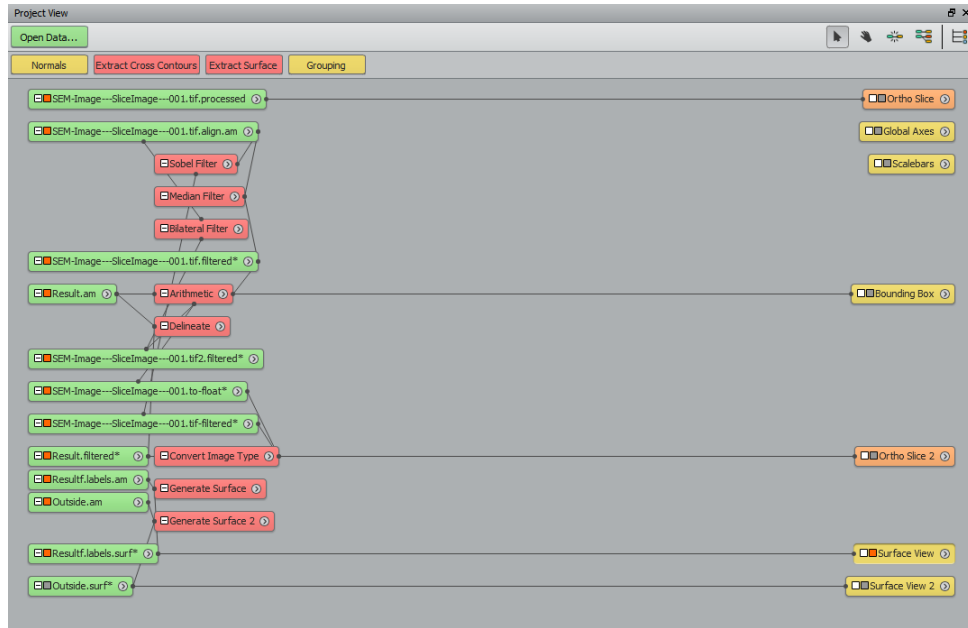


Figure 4: Order of Composite Filter Operations

2.4 Image Segmentation

Image segmentation is carried out in the *Segmentation Editor* (Figure 5). This process assigns a label to each pixel of the image, which describes the material associated with

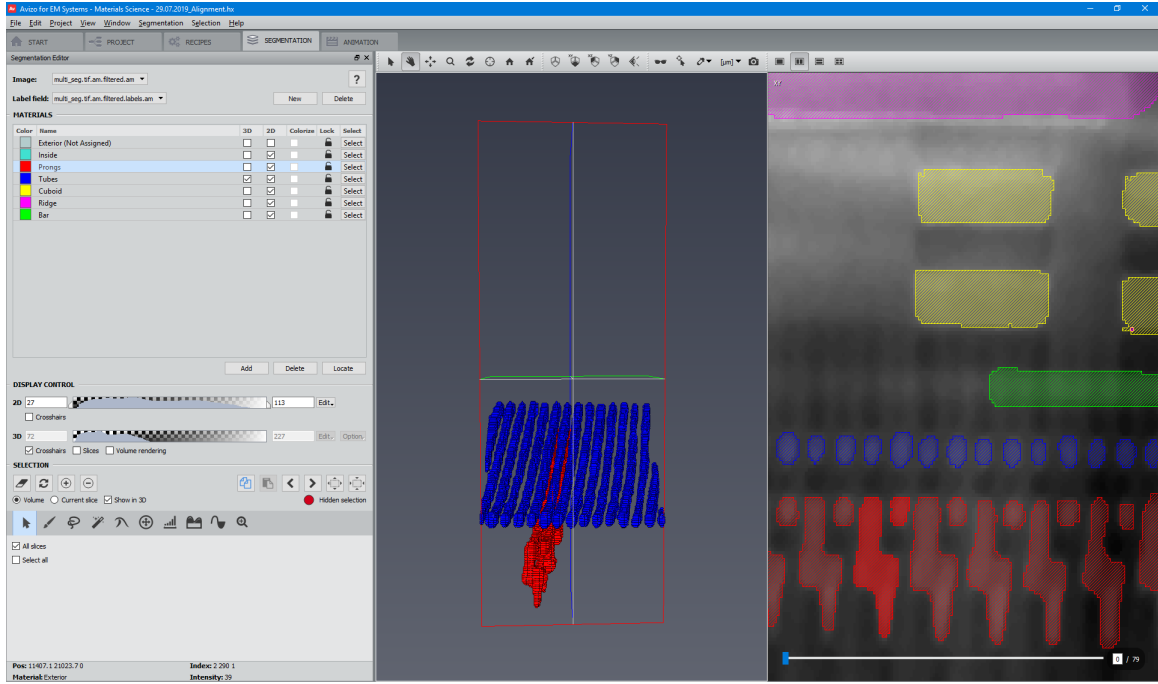


Figure 5: Segmentation Editor

the pixel. The segmentation is stored in a separate data object called a Label Field. Segmentation is a prerequisite for surface model generation and accurate quantification such as volume measurement.

The following Segmentation tools are found under the *Selection* area of the *Segmentation Editor*, and are used in combination to individually select the various components/materials of the microchip (Figure 6). Voxels of the same gray value are indicative that the materials are the same.

1. *Brush*: Manually select voxels. Very slow, but accurate.
2. *Lasso*: Allows the user to define an area by generating a closed contour curve in 2D or 3D. Freehand mode (2D) is useful for making selections of an irregular shape.
3. *Magic Wand*: Uses a region growing operation. Seed point is manually selected by clicking a voxel. This tool then auto-selects all adjacent voxels with gray values within a user-defined range. This range is set in the *Masking* slider. Fast, but not very accurate.
4. *Blow*: When a voxel is selected by clicking, the user drags the mouse without releasing the button, generating a initially circle-shaped contour expands. The greater the distance from the initial position of the mouse click, the more the contour grows. The contour grows in areas with homogeneous gray values and to stop where gray values change abruptly.
5. *Threshold*: Uses a contrast threshold filter to select voxels of similar gray value.

6. *Top-hat*: Detects dark or light areas in the image, corresponding to the valleys or the narrow peaks of a function f , using morphological operators. Very fast, quite accurate.



Figure 6: Segmentation Selection Tools

The *Interpolate* function interpolates the selection between all slices where areas have been selected. Interpolation is done along one orientation, defined by the 2D viewer in use. This tool is prone to error, and often requires correction. It is therefore recommended that the user views the sample through multiple views, and manually scans through the selected slices prior to adding them to the Label Field of a material. Errors can be corrected using the *Brush* tool.

After selection, the voxels are assigned to a material in the *Materials* area of the *Segmentation Editor*.

In the *Project View*, the Label Field data is generated as a module ending in “.labels.am”. The reconstructed sample is displayed *Viewer* using the **Surface View** or **Volume Rendering** modules.

The generated 3D surface is analysed and various properties determined using the **Volume Fraction** module, and components of interest measured using the *Measure* tool.

3 Results & Analysis

Five distinct components were identified in the sample and distinguished using the Segmentation tools in the *Segmentation Editor*.

Component names, “Tubes”, “Bar”, “Ridge”, “Cuboid” and “Prongs” were chosen arbitrarily. Due to the limitations of gray value similarity, the composition of these components could not be determined. However, due to the observance of a continuum of repeated structures through the microchip, the distinction between these five structural components of the microchip was deemed worthwhile. The fully reconstructed 3D image is shown in Figure 7 and Figure 8.

3.1 Features of Interest

The 3D reconstruction allowed several features of the microchip to be identified in significant detail. The “tubes” (blue in Fig. 7, 8) were observed to be long uninterrupted tubes of diameter 270 ± 30 nm. The “prongs” (red in Fig. 7, 8), are alternating prongs that are interconnected in pairs, with opposite chirality (Figure 9). Each “prong” has a height of $\approx 1.3 \mu\text{m}$, width $\approx 0.40 \mu\text{m}$ and thickness ≈ 40.0 nm.

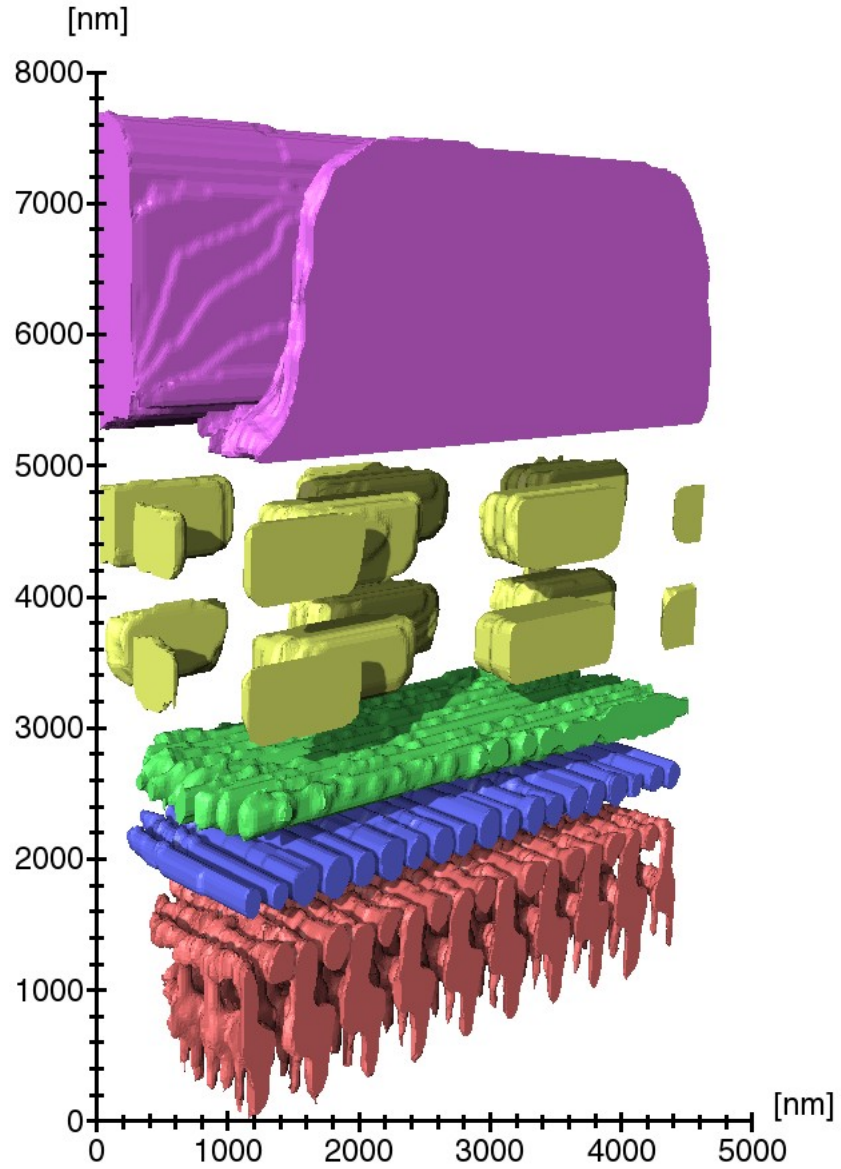


Figure 7: **Surface View** of the Microchip, indicating 5 distinct components.
 Key: Pink = Ridge. Yellow = Cuboid. Green = Bar. Blue = Tubes. Red = Prongs

3.2 Volume Fraction V_f

The volume fraction V_f of each component was obtained using the **Volume Fraction** module, which outputs a spreadsheet with data that can be used to plot a graph of volume fraction vs material (Figure 10). However, the plot produced is limited insofar

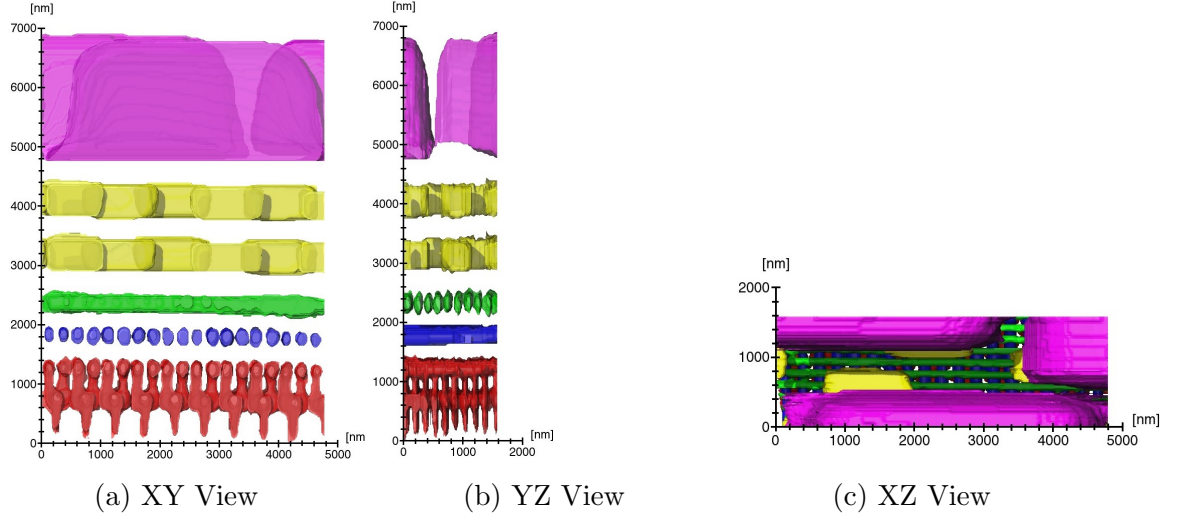


Figure 8: **Surface View** of the Microchip from the XY, YZ, AND XZ views respectively.
Key: Pink = Ridge. Yellow = Cuboid. Green = Bar. Blue = Tubes. Red = Prongs

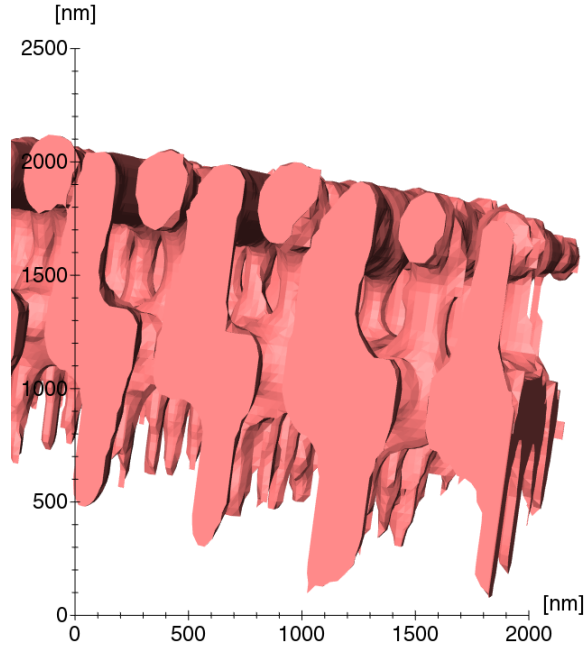


Figure 9: Component of the microchip, "Prongs". The alternating chiral pairs are apparent in the image above.

as the computed V_f of each material is the volume fraction relative to the volume of the entire bounding box and not relative to the volume of the sum of the 3D reconstructed components.

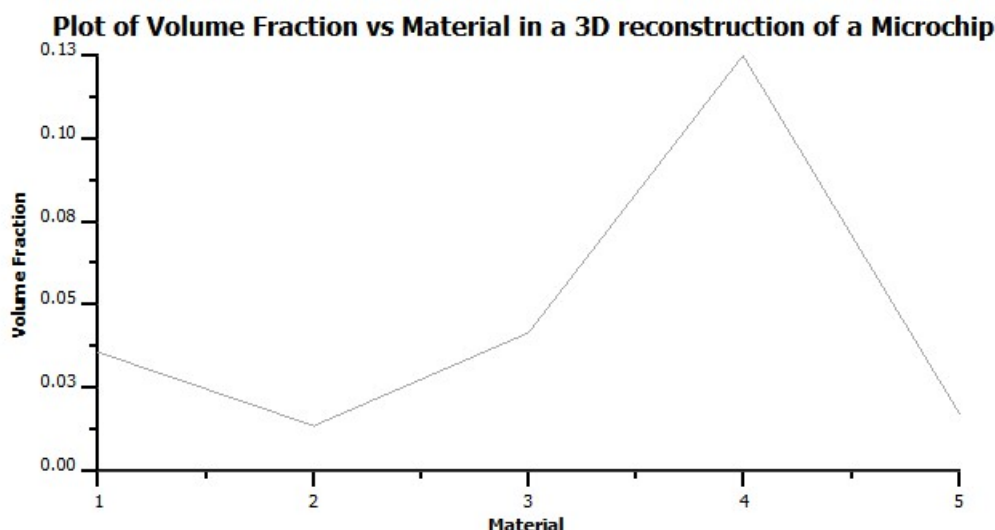


Figure 10: Plot indicating the volume fraction of each material in the microchip sample.
Key: 1 = Prongs. 2 = Tube. 3 = Cuboid. 4 = Ridge. 5 = Bar.

3.3 Application to an Larger Sample

The above procedure was repeated for an additional sample, this time in a different section of the microscope, and with 500 slices. The resultant reconstruction was successful, showing that this is a widely applicable technique, in which the same algorithms can be applied to reconstruct various samples successfully. The elemental indications given in Figures 11 and 12 were provided by EDX analysis at the DESY NanoLab, coupled with X-ray scattering experiments on the P06 beamline at Petra, DESY. However, these data are not fully integrated into the 3D reconstruction and can be interpreted as a rough indication only. Furthermore, the exact molecular structure of the compounds has yet to be integrated into the reconstruction.

3.4 Limitations

The technique of Image Segmentation as described was quite time consuming as it is intrinsically limited by the contrast of the components within the images. The *Magic Wand* tool speeds up this process, but is unable to manage more than small sections of the sample at once. The *Interpolate* selection filter was also very error prone for this dataset. Additional steps in image processing to increase the contrast between grey values could allow for greater speed and accuracy in the Image Segmentation stage.

Furthermore, due to varying grey level ranges at different sections of the microchip, fidelity could be increased by reconstructing these different sections of the microchip independently, and later stitching the reconstructed parts together.

Due to the extensive time consumption of “manual” Image Segmentation, investigations into an automated segmentation process are of interest. A potential solution to this problem could involve the use of an algorithm that filters selected particles by their size.

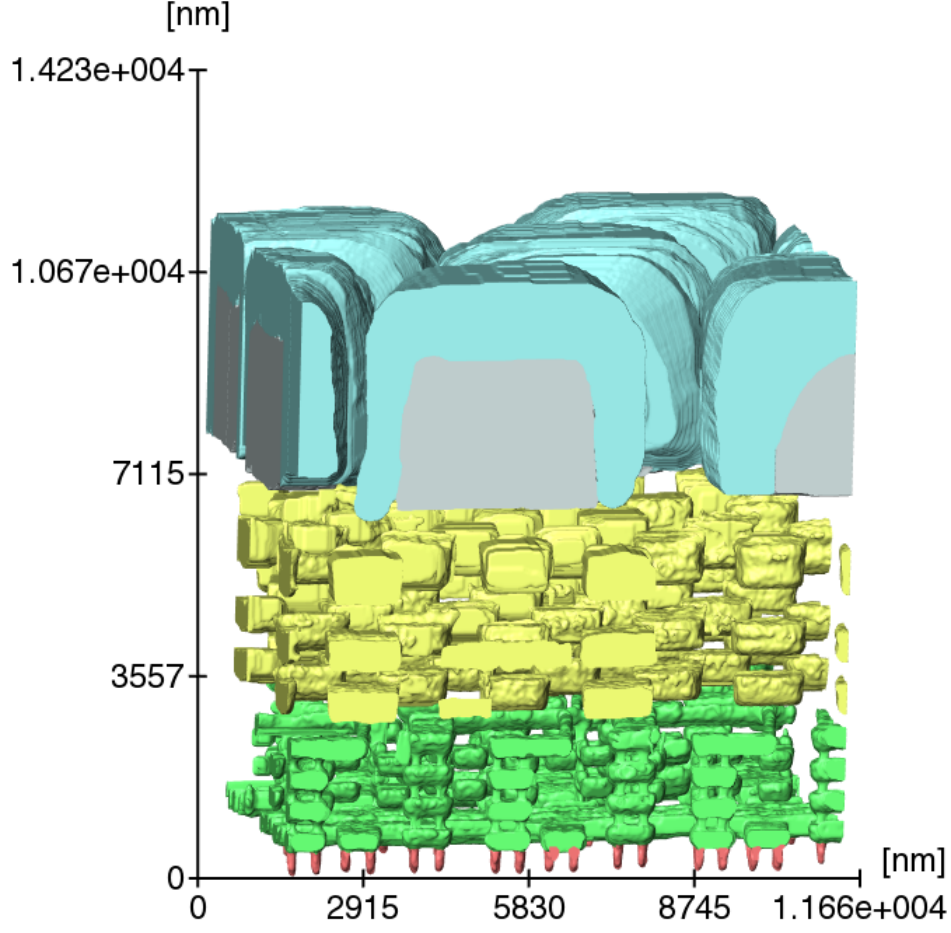


Figure 11: Surface View of the Microchip, indicating 5 distinct components.

Key: Silver = Al. Blue = Si and O compound. Yellow, Green = Cu, Ta compound. Red = W

4 Conclusions and Outlook

The Image Segmentation method in *Avizo* has been generally successful in the 3D reconstruction of the interior components of the microchip. Five distinct components were identified and their properties measured in *Avizo*. The initial 3D reconstruction showed an angular drift of 52° , the same angle as of that between the FIB and the SEM. This was rectified successfully in subsequent reconstructions by the alignment method described. This was shown to work as the microchip plane was parallel to the X-axis.

Furthermore, the method described was limited by its time-intensity. The incorporation of an algorithm that filters segmentation by size should be explored in future reconstructions. Moreover, 3D reconstruction of this kind is limited by its inability to ascertain details of the chemical composition of the sample. A comprehensive approach, inclu-

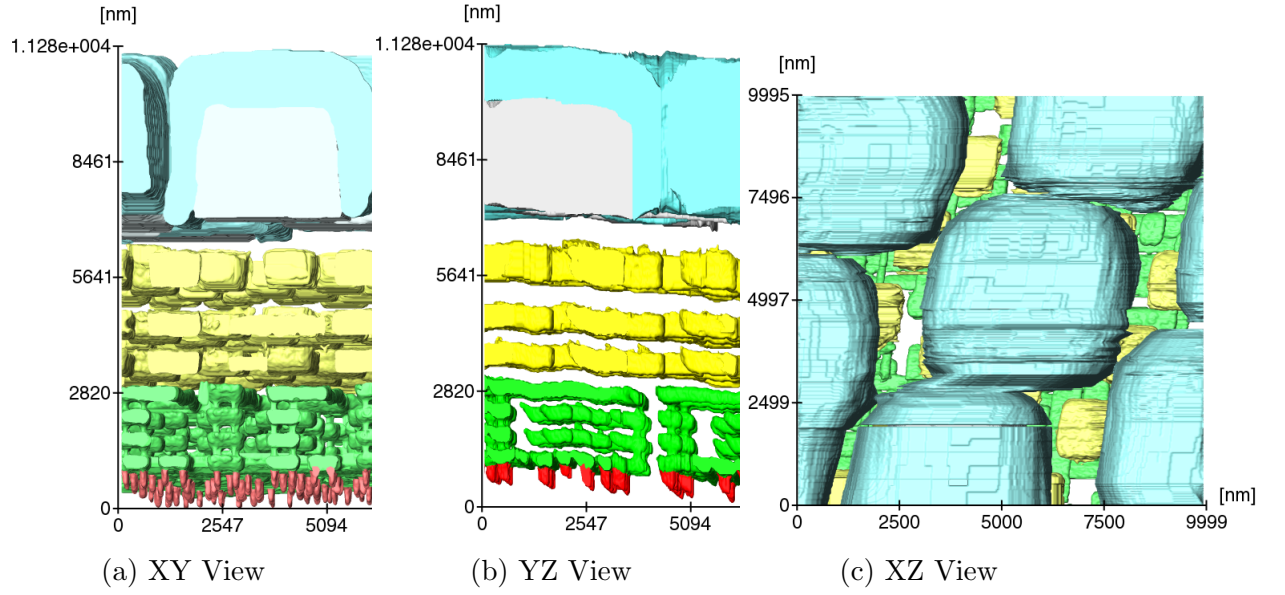


Figure 12: **Surface View** of the Microchip from the XY, YZ, AND XZ views respectively.

Key: Silver = Al. Blue = Si and O compound. Yellow, Green = Cu, Ta compound. Red = W

sive of both 3D reconstruction as well as Energy-Dispersive X-ray spectroscopy (EDX), should yield an accurate description of both the physical and chemical composition of the materials in the sample.

References

- [1] Fei.com, 2019. [Online]. Available: <https://www.fei.com/software/avizo/?LangType=2052>. [Accessed: 02- Sep- 2019]. *FEI Website*.